Title
Conceptual design of beam-ion profile diagnostics for the DIII-D tokamak

Journal
Review of Scientific Instruments, 74(3)

ISSN
0034-6748

Authors
Heidbrink, WW
Cross, WD
Krasilnikov, AV

Publication Date
2003-03-01

DOI
10.1063/1.1534399

Conceptual design of beam-ion profile diagnostics for the DIII-D tokamak

W. W. Heidbrink[a] and W. D. Cross
University of California, 4129 Frederick Reines Hall, Irvine, California 92697-4575

A. V. Krasilnikov
Troitsk Institute of Innovating and Fusion Research

(Presented on 9 July 2002)

Three diagnostic concepts that measure the radial profile of deuterium beam ions are assessed. One diagnostic exploits 3 MeV protons that are lost on their first orbit. Since beam-plasma reactions usually predominate in the discharges of interest, the beam-ion density profile can be inferred from the *d-d* fusion reaction profile. The relatively modest plasma current ($\sim$1.6 MA) implies that a significant fraction of the charged *d-d* fusion reaction products are unconfined. The second diagnostic employs a neutron collimator. For this diagnostic, neutron scattering is a major concern. Both fusion product diagnostics are sensitive to uncertainties in the thermonuclear rate, so the anomalous beam-ion transport must exceed $D_B \gtrsim 1.0\ \mathrm{m}^2/\mathrm{s}$ to be detectable. The third diagnostic employs an array of natural diamond detectors that is configured to measure the signal from beam ions that charge exchange with neutrals in a modulated heating beam. The sensitivity to uncertainties caused by pitch-angle scattering of the beam ions can be minimized by a prudent choice of detection angle. Because of attenuation of the escaping neutrals the effective resolution is $D_B \sim 0.5\ \mathrm{m}^2/\mathrm{s}$. [DOI: 10.1063/1.1534399]

I. INTRODUCTION

Calculations based on classical beam-ion confinement often overestimate the measured pressure profile and neutron rate, particularly in DIII-D advanced tokamak (AT) plasmas with beam-driven Alfvén activity.[1] Knowledge of the beam-ion profile is crucial for confinement studies, for current-drive studies, for calculations of magnetohydrodynamic (MHD) stability, and for studies of fast-ion driven instabilities. Measurement of the entire beam-ion distribution function $f_b(\mathbf{v},\mathbf{r},t)$ is desirable but, in practice, the radial dependence of f_b is of the greatest importance. Beam deposition is strongly peaked on axis and the velocity-space dependence of the distribution function is governed primarily by Coulomb scattering,[2] so anomalous spatial transport is easier to detect than anomalous velocity-space transport. Moreover, for several applications (such as MHD stability calculations), only knowledge of the beam pressure gradient is required. Our objective is a diagnostic that measures the radial profile of the beam-ion density $n_b(r)$ with a spatial resolution that can resolve differences in anomalous beam-ion diffusion of $D_B \simeq 0.3\ \mathrm{m}^2/\mathrm{s}$.

Five diagnostic systems are under consideration: A 2.5-MeV neutron collimator; a 3 MeV proton pinhole camera; an active charge-exchange array; a microwave collective scattering diagnostic; and D_α light emitted by reneutralized (''halo'') beam ions. This article evaluates idealized versions of the first three techniques. The baseline discharge for this evaluation is an extensively studied[3] AT discharge (#99411) with anomalous fast-ion transport. The TRANSP code[4] can include an *ad hoc* diffusion coefficient in its calculation of the beam-ion profile; the sensitivity of the signals to variations in D_B is a useful figure-of-merit. Uncertainties associated with dependencies on other plasma parameters imply that the resolution in D_B is likely to exceed 0.5 m^2/s for all three techniques (Table I).

II. NEUTRON COLLIMATOR

Although thermonuclear rates are appreciable, most of the fusion reactions in a typical AT plasma involve beam ions, so, in principle, the beam-ion profile can be inferred from the fusion reaction profile. Massive neutron collimators were designed with the facility and gave excellent results on the Tokamak Fusion Test Reactor (CTFTR) and the Joint European Torus (JET).[2] Except for a reinforced pad directly underneath the machine, the soil beneath DIII-D cannot bear appreciable loads, so a massive collimator requires expensive engineering. Chords from an affordable $3.0\times1.7\times2.0\ \mathrm{m}^3$ collimator on the reinforced pad is illustrated in Fig. 1(a). A major concern in any spatially resolved neutron measurement is the signal from neutrons that scatter off structural elements into the sightline. Sightlines through vacuum ports minimize backscattering for two off-axis chords. The geometry for a central chord is less favorable but, because the signal is larger, scattering into the sightline (not calculated yet) and attenuation of the virgin neutrons in the graphite tiles and stainless steel flange ($\sim$42%) may be tolerable.

An assessment of an idealized version of this array is shown in Fig. 2. The calculated TRANSP fusion emissivity profiles for various values of D_B are shown in Fig. 2(a). Figure 2(b) shows the ideal signals for the three collimator sightlines as a function of D_B; the spatial resolution is assumed perfect (pencil-beam approximation) and scattered neutrons are neglected. Even for a perfect neutron detector,

[a]Electronic mail: wwheidbr@uci.edu

TABLE I. Comparative assessment of beam-ion profile diagnostics.

Technique	Technical hurdle	Plasma	Resolution[a] (m^2/s)
2.5 MeV neutron	scattering	D^0 Neutral Beam Injection (NBI)	1.0
3 MeV proton	-	D^0 NBI; $I_p \lesssim 1.6$ MA	1.0
45 keV neutral	in-vessel NDD	$n_e \lesssim 5\times10^{19}$ m^{-3}	0.5

[a]For the baseline discharge.

uncertainties in thermal deuterium density and temperature cause ~30% uncertainty in the thermonuclear rate for this base-line case, which implies an ~10% uncertainty in the expected signal. These uncertainties alone are comparable to the expected variation associated with beam diffusion for $D_B \leqslant 1.0$ m^2/s.

III. PROTON PINHOLE CAMERA

Relative to neutron diagnostics, an advantage of charged fusion product measurements is that the short range of charged ions permits small collimators and effectively eliminates scattered particles as a source of noise; the corresponding disadvantage is that the detectors must be placed within the vacuum vessel. A second disadvantage is that charged fusion products escape on curved orbits, while neutrons travel in straight lines. DIII-D has an excellent Motional Stark Effect diagnostic[5] that provides the data required to obtain accurate equilibrium reconstructions,[6] so the trajectory of the escaping fusion products is no longer a major uncertainty in most AT plasmas. In high-current plasmas ($I_p \gtrsim 1.6$ MA), the proton orbits become very sensitive to the poloidal field (most protons are confined) and the resolution deteriorates.

Zweben used a pinhole camera with a scintillator detector to measure charged fusion products in TFTR.[7] Figure 1(b) shows 3 MeV proton orbits into a detector at the bottom of DIII-D for the baseline case. The toroidal angle of the proton velocity vector at the scintillator determines the measured trajectory. Conceptually, the detector functions as a pinhole camera with the additional complication that the measured sightlines are curved. Unfortunately, the spatial resolution of the ''sightline'' is determined by the radial width of the orbit, which is given by the ~20 cm gyrodiameter of the 3 MeV protons.

An ideal camera is sensitive to beam-ion diffusion [Fig. 2(c)]. There are several factors that degrade the potential sensitivity of the measurement, however. The most important of these is the sensitivity to uncertainty in the thermonuclear rate [shown in Fig. 2(c)]. Uncertainties associated with possible systematic errors in the equilibrium reconstruction are at the 5%–10% level. Doppler broadening of the 3 MeV proton source causes a spread of about 10% in birth energy for the protons (for beam-plasma reactions), but the associ-

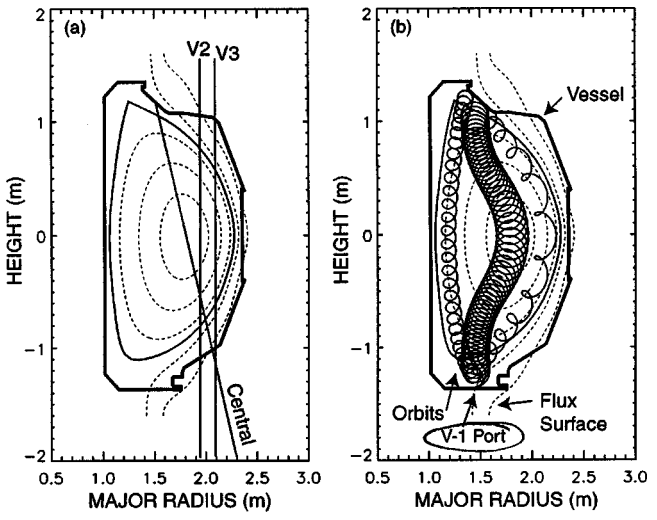

FIG. 1. Elevation of DIII-D showing the vacuum vessel (thick solid line) and flux surfaces (dotted) for discharge #99411. (a) Neutron collimator chords. The V2 and V3 chords pass through thin flanges but the central chord intersects the vacuum vessel at two locations. (b) Three of the proton orbits ''viewed'' by a pinhole camera in the V-1 port. From the outer major radius to the inner, the toroidal angle of the velocity vector for these three orbits is −56°, −8°, and 56°.

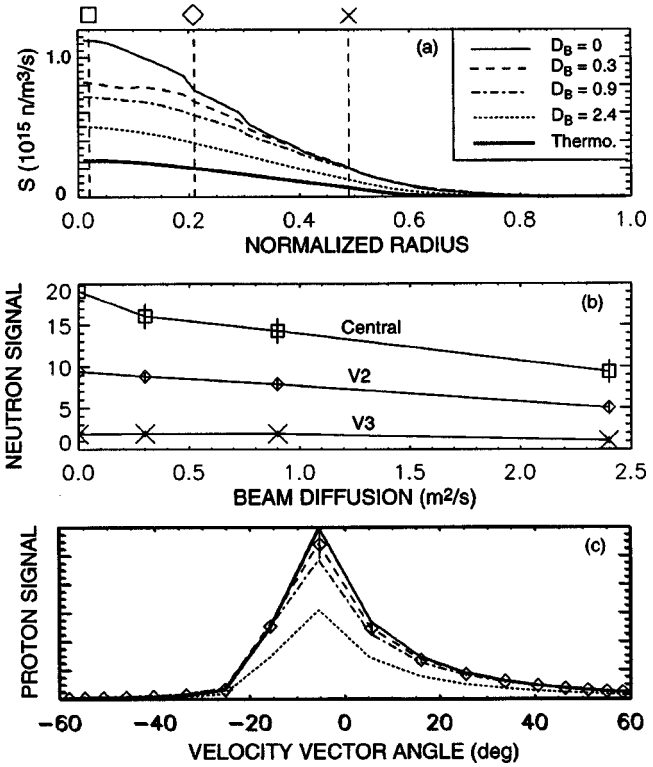

FIG. 2. (a) Fusion emissivity vs normalized square root of the toroidal flux ρ for various values of the beam-ion diffusion coefficient D_B (in m^2/s) for discharge #99411 at 1.8 s. The contribution from thermonuclear reactions is also shown (thick solid line). The dashed vertical lines represent the minimum ρ of each chord. (b) Calculated neutron signals $\int S\,dl$ for the ideal chords shown in Fig. 1(a). (c) Calculated proton signals $\int S\,dl$ vs toroidal angle of the velocity vector for the pinhole camera shown in Fig. 1(b). In (b) and (c), the error bars represent the uncertainty caused by 30% uncertainty in the thermonuclear rate.

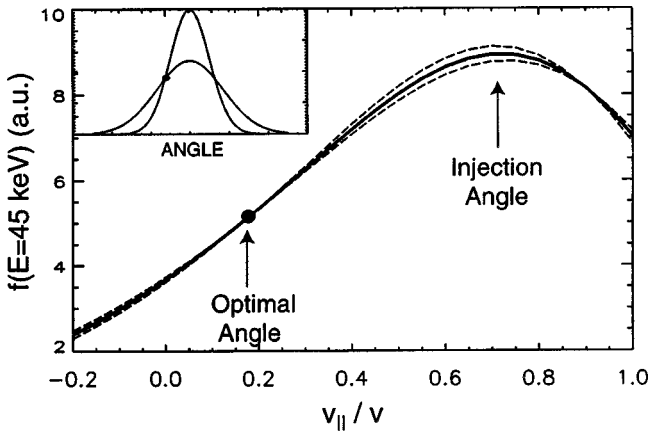

FIG. 3. Local calculation[10] of the steady-state beam ion distribution function $f_b(E,v_\parallel/v)$ vs pitch of detection for near-tangential (''left'') beam injection. The dotted lines indicate the variation in f_b caused by variations in Z_{eff} of $\pm 10\%$. (Typical uncertainties are larger.) At an optimal angle, the sensitivity to uncertainty in Z_{eff} is eliminated. The inset illustrates diffusive spreading of an initially peaked distribution in one dimension. Although the peak value of the distribution and the far wings of the distribution depend sensitively on the diffusion coefficient, for the particular value of the abscissa marked with a solid dot, the ordinate is independent of the diffusion coefficient.

ated error is only $\lesssim 2\%$. The angular resolution at the scintillator approaches 2° in recent instruments,[8] so this is a negligible source of error. The equivalent resolution of the proton camera is $D_B \sim 1.0\ \text{m}^2/\text{s}$ in AT plasmas with appreciable thermonuclear emission. For both fusion-product techniques, measuring the energy as well as the flux could discriminate against thermonuclear fusion products and improve the equivalent resolution.

IV. NEUTRAL PARTICLE ARRAY

The plasma emits energetic neutrals when beam ions exchange an electron with injected neutrals. If the source of injected neutrals is modulated (''active charge exchange''), analysis of the escaping neutrals provides spatially resolved information about $f_b(E,v_\parallel/v,\mathbf{r})$, where E and $v_\parallel/v$ are the energy and pitch of the neutral. With enough measurements of f_b, the beam density $n_b(r)$ can be determined. In contrast

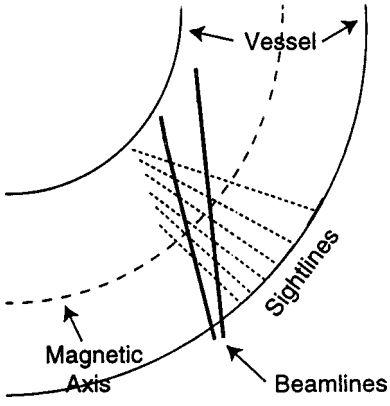

FIG. 4. Plan view of a sector of the DIII-D vessel showing the angle of injection of the two heating beams (solid) and the orientations of the sightlines that minimize the sensitivity to uncertainties in Z_{eff}. Diamond detectors placed behind collimating holes in the graphite tiles detect the neutrals.

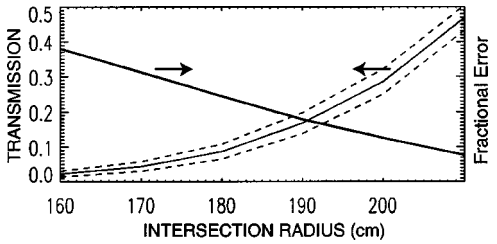

FIG. 5. Product of the transmission of 80 keV neutrals injected by the heating beam and transmission of 45 keV escaping neutrals as a function of the radius of the intersection of the sightline with the heating beam for the sightlines illustrated in Fig. 4. The dotted lines represent the transmission for $\pm 10\%$ changes in electron density (a typical error). The fractional uncertainty in transmission is very large for the interior sightlines.

to fusion product measurements, which effectively perform a weighted average over the velocity dependence of f_b, neutral particle measurements are local in phase space. To use local measurements of f_b to infer the total density n_b, either many measurements or prudent selection of E and $v_\parallel/v$ are required.

A population of injected beam ions decelerates in energy and diffuses in pitch. Sensitivity to anomalous spatial transport is maximized by measuring low energies; in practice, an energy just above the energy of newly injected half-energy beam ions ($\sim$45 keV in DIII-D) is best. The pitch-angle scattering rate is proportional to the effective charge Z_{eff}, which can have substantial uncertainties. A low rate implies a peaked angular distribution, while a fast rate implies a broad distribution. At a certain measurement angle, however, the sensitivity to uncertainties in pitch-angle scattering are minimized (Fig. 3). An array that uses the heating beams as modulated sources of neutrals and measures the optimal pitch-angle for the conditions of our baseline discharge is shown in Fig. 4. In contrast, a conventional pinhole array through a single port is far too sensitive to uncertainties in Z_{eff} for a useful beam-ion profile diagnostic.

The sightlines shown in Fig. 4 do not correspond to available diagnostic ports, precluding the use of conventional neutral particle analyzers. One possibility is to use 50-μm-thick natural diamond detectors (NDD)[9] that are mounted behind small holes in the graphite tiles. Electronic noise and a background neutron signal that is comparable to the desired signal may preclude pulse counting in this harsh environment; if energy resolution is sacrificed, current-mode operation is one possible solution.

Another difficulty is attenuation of the injected neutral beam and of the escaping neutrals. To infer the beam density from the measured signals, a correction for attenuation is required. This correction factor is quite sensitive to uncertainties in electron density for high densities and for long path lengths (Fig. 5). For the baseline discharge, this uncertainty implies an achievable resolution of $D_B \simeq 0.5\ \text{m}^2/\text{s}$.

ACKNOWLEDGMENTS

Discussions with R. Boivin, D. Darrow, and M. Murakami and neutron calculations by D. Prosvirin and V. Khripunov are gratefully acknowledged. This work was

funded by General Atomics Subcontract No. SC-G903402 under U.S. Department of Energy Contract No. DE-AC03-99ER54463.

[1] W. W. Heidbrink, E. Ruskov, E. M. Carolipio, J. Fang, M. A. van Zeeland, and R. A. James, Phys. Plasmas **6**, 1147 (1999).
[2] W. W. Heidbrink and G. J. Sadler, Nucl. Fusion **34**, 535 (1994).
[3] M. Murakami, M. S. Chu, J. C. DeBoo, C. M. Greenfield, J. E. Kinsey, L. L. Lao, R. J. LaHaye, Y. R. Lin-Liu, T. C. Luce, P. A. Politzer, B. W. Rice, G. M. Staebler, T. S. Taylor, M. R. Wade, and DIII-D Group, Nucl. Fusion **40**, 1257 (2000).
[4] R. V. Budny, Nucl. Fusion **34**, 1247 (1994).
[5] B. W. Rice, D. G. Nilson, and D. Wroblewski, Rev. Sci. Instrum. **66**, 373 (1995).
[6] L. L. Lao, H. St. John, R. D. Stambaugh, A. G. Kellman, and W. P. Pfeiffer, Nucl. Fusion **25**, 1611 (1985).
[7] S. J. Zweben, Nucl. Fusion **29**, 825 (1989).
[8] D. S. Darrow, A. Werner, and A. Weller, Rev. Sci. Instrum. **72**, 2936 (2001).
[9] A. V. Krasilnikov, S. S. Medley, N. N. Gorelenkov, R. V. Budny, D. S. Darrow, and A. L. Roquemore, Nucl. Fusion **39**, 1111 (1999).
[10] R. J. Goldston, Nucl. Fusion **15**, 651 (1975).